Dynamic assessment of a FRP suspension footbridge through field testing and finite element modelling

Dynamic assessment of a FRP suspension footbridge through field testing and finite element modelling

Renos A. Votsis[*1a], Tim J. Stratford[2], Marios K. Chryssanthopoulos[3] and Elia A. Tantele[1]

[1]*Department of Civil Engineering and Geomatics, Cyprus University of Technology, Saripolou street 2-8, Achilleos Building 1, Floor 1, 3603 Limassol[1], Cyprus*
[2] *School of Engineering, University of Edinburgh, U.K.*
[3]*Civil Engineering (C5), Faculty of Engineering and Physical Sciences, University of Surrey, U.K.*

Abstract. The use of advanced fibre composite materials in bridge engineering offers alternative solutions to structural problems compared to traditional construction materials. Advanced composite or fibre reinforced polymer (FRP) materials have high strength to weight ratios, which can be especially beneficial where dead load or material handling considerations govern a design. However, the reduced weight and stiffness of FRP footbridges results in generally poorer dynamic performance, and vibration serviceability is likely to govern their design to avoid the footbridge being "too lively".

This study investigates the dynamic behaviour of the 51.3m span Wilcott FRP suspension footbridge. The assessment is performed through a combination of field testing and finite element analysis, and the measured performance of the bridge is being used to calibrate the model through an updating procedure.

The resulting updated model allowed detailed interpretation of the results. It showed that non-structural members such as the parapets can influence the dynamic behaviour of slender, lightweight footbridges, and consequently their contribution must be included during the dynamic assessment of a structure. The test data showed that the FRP footbridge is prone to pedestrian induced vibrations, although the measured response levels were lower than limits specified in relevant standards.

Keywords: fibre reinforced polymer; footbridges; vibration serviceability; finite element method; dynamic test

1. Introduction

The quest for lighter, corrosion-resistant and pre-fabricated structures has fuelled growth in the use of fibre reinforced polymer (FRP) materials in bridge construction (Bakis *et al*. 2002, Keller 2003). In Europe, all-FRP composites bridge solutions (as opposed to applications of FRPs for strengthening or deck replacement) were first applied to pedestrian bridges, followed in the past decade by highway bridges. Early applications of FRP footbridges included crossings in remote inaccessible areas (capitalising upon the material's light weight for easy installation) or as walkways in harsh environments and industrial plants (Hollaway and Head 2001). More recently, whole-life considerations such as an anticipated reduction in maintenance costs have driven the use of FRP bridges. The reduction in weight and the modern tendency for slender construction

[*] Corresponding author, PhD, Email: rvotsis@gmail.com; renos.votsis@cut.ac.cy

forms (SETRA 2006), however, make careful consideration of the vibrational behaviour (including human-structure interaction) especially important.

Footbridges can suffer from noticeable vibration independently of their structural form or construction material. Investigations into footbridges that have "lively" behaviour have shown that these structures have similar natural frequencies. For vertical vibration, vibration problems occur within the frequency range 1.5 to 2.5Hz, whereas in the horizontal direction, the problematic range is 0.5 to 1.1Hz (Pimentel 1997, Zivanovic *et al.* 2007). Some footbridges only experience problems after they are loaded with heavy pedestrian traffic, as was the case for the London Millennium footbridge (Dallard *et al.* 2001). Low damping can also contribute to poor dynamic performance, with steel footbridges exhibiting the lowest values (Hivoss 2008).

Vibrations can be problematic due to resonance, when the frequency of the excitation is close to the frequency of the structure. For pedestrian loading, a vertical fluctuating force ranging from 180N (BS5400 2006) to 280N (EN1995 2004, Barker *et al.* 2005) is created during walking, which is repeated with each step. Normal pacing rates are 1.4 to 2.4Hz (Matsumoto *et al.* 1978, Pachi and Ji 2005), though higher frequencies of up to 5Hz can be achieved by the second harmonic of walking and running (Bachmann 2002, Willford 2002). Walking also creates smaller dynamic forces (25N) in the horizontal direction, with an excitation frequency approximately half the walking frequency (Fujino *et al.* 1993).

Therefore the natural frequencies of footbridges should ideally lie outside the above frequency ranges to avoid resonance. This is not always practicable, however, in which case the dynamic behaviour of the footbridge must be assessed in more detail. For example, international standards (FIB 2005) suggest serviceability checks for footbridges having vertical frequencies less than 5Hz (critical ranges 1.5 to 2.4Hz and 3.5 to 4.5Hz) or horizontal frequencies less than 2.5 Hz (critical range 0.8 to 1.2Hz).

The footbridge investigated in this paper belongs to a small group of bridges with decks built entirely from FRP material. Similar bridges include the Halgavor and the Aberfeldy footbridges in the UK, the Kolding in Denmark, the Lleida in Spain and the Chertanovo in Moscow. At present, knowledge about the dynamic performance and properties of such bridges is limited (Alampalli and Washer 2013), and thus physical testing provides valuable information for future similar structures, in terms of natural frequencies, mode shapes and damping. Measurements of damping are particularly useful as it cannot be estimated by prior theoretical or numerical analysis. This paper describes in-situ measurement of response of Wilcott footbridge to pedestrian crossings, giving beneficial data on its dynamic performance. The field test results have also been used to calibrate a finite element (FE) model of the bridge, which allowed the stiffness of components such as the GFRP bridge deck and the steel suspension cables to be deduced, and which demonstrated that the parapets can significantly affect the footbridge's stiffness. Such a model can be used for asset management purposes and for the design of future similar structures.

2. Description of the Wilcott Footbridge

The Wilcott footbridge is located in Shropshire, UK and was opened in March 2003. It connects the villages of Wilcott and Nesscliffe, which are separated by the A5 dual carriageway road. It is a 51.3m single span suspension footbridge with a slightly cambered 2m wide deck (Cadei 2003). A general view of the bridge can be seen in Fig. 1.

Fig. 1 An overview of the completed Wilcott footbridge.

The main feature of the bridge is the glass fibre reinforced polymer (GFRP) deck. It was fabricated from the Advanced Composite Construction System (ACCS) which is pultruded by Strongwell Corp under the trade name Composolite (Strongwell 2010). The same system was previously used on the Aberfeldy footbridge, a 63m span cable-stayed bridge constructed in 1992 (Stratford 2012). The ACCS is a modular system comprising standard pultruded components that are connected together by adhesive bonding, with a mechanical interlock "toggle" connection that provides location and support whilst the adhesive cures. The Wilcott footbridge deck is shown in Fig. 2, and Fig. 3 shows part of the deck during fabrication (before closing the box). The transverse cross-beams visible in Fig. 3 are located where the hanger cables are connected to the bridge deck, as well as at every parapet post (see Fig. 1). The GFRP deck was prefabricated in three equal parts which were later assembled on-site. It is topped by interlocking rubber blocks manufactured from recycled vehicle tyres.

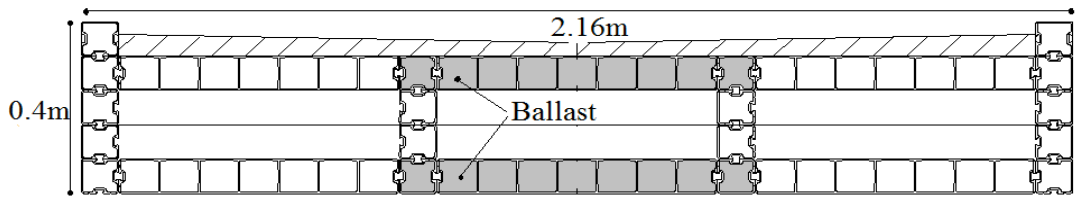

Fig. 2 A cross-section through the bridge deck.

Fig. 3 Fabrication of the GFRP bridge deck, showing the configuration of the transverse beams.

The bridge has a spiral strand steel cable system (for both the main suspension cables and hangers), supported from steel circular hollow section pylons, which are anchored using solid Macalloy steel bar backstays. The inclined hangers are connected to the deck using a stainless steel plate backed by four threaded studs bonded into the end of the cross beam, and to the main cables with steel clamps. The bridge is supported at the abutments by two concrete raft foundations, which connect the bridge deck (cast into pockets in the concrete), the pylon support plinths, and the backstay connection plinths.

Two features are of particular note to the dynamic performance of the bridge. The first is that the central panels of the deck were ballasted (using mortar blocks sized so that they could slide into the cells), as shown in Fig. 2. The ballast was intended to increase the mass of the deck; placing it near the centre-line of the deck helped separate the vertical and torsional vibration natural frequency. The parapet system is also worthy of description; this consists of stainless steel parapet posts, with connecting handrails and footrails that contain joints that allow longitudinally extension. A stainless steel cable mesh system is attached to the parapets.

3. Finite Element Modelling

Finite element modelling was used to provide greater insight into the behaviour of the structure, both prior to the field test and to help interpret the measured results. Wilcott footbridge was modelled using the ANSYS commercial finite element program (ANSYS 2003). A three dimensional (3D) FE model was created, as shown in Figs. 4-5. The composite deck was modelled in detail using shell elements and the functionality of the parapets was represented by spring elements. Modelling these parts separately allowed detailed comparison with the footbridge's actual behaviour.

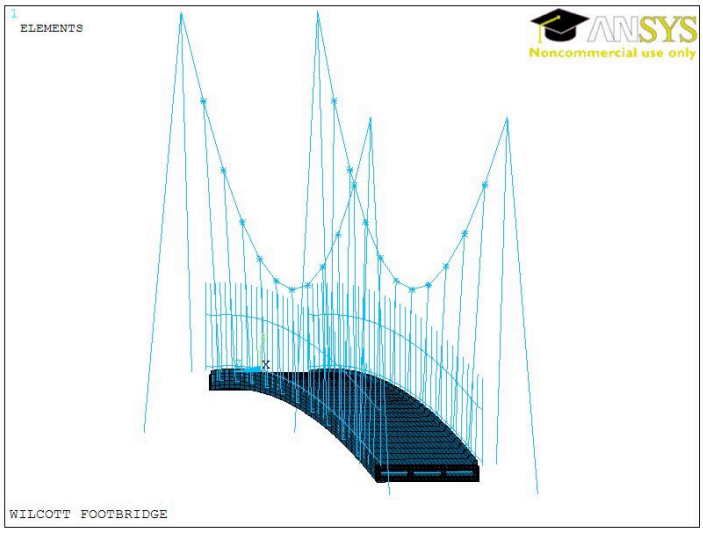

Fig. 4 An overview of the finite element model of the bridge.

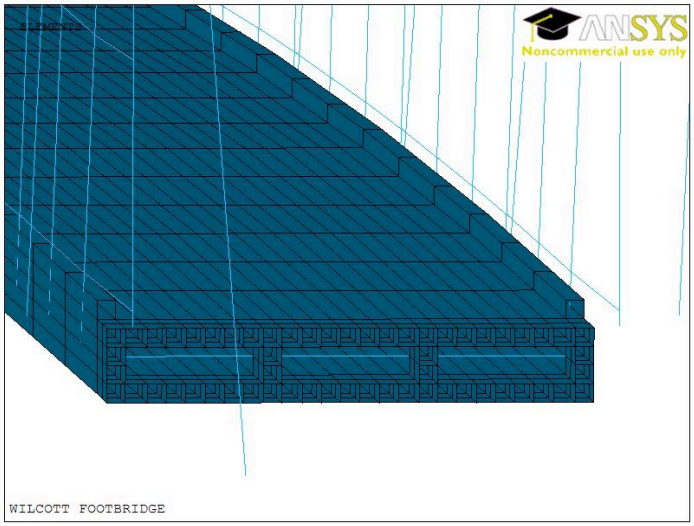

Fig. 5 A detailed view of the GFRP modular deck within the model.

3.1 FE Model description

The composite deck was modelled using anisotropic 8-noded shell elements (shell93), as shown in Fig. 5. The cross-beams were modelled using beam elements (beam4) of equivalent stiffness within the cellular box of the deck, so as to simplify the model and reduce the computational requirements. The ballast was included as a distributed mass; any potential minor contribution to the structural stiffness was neglected.

The main suspension cables, the hanger cables and the backstays, were all modelled as tension only (truss) elements (link10), which have stress-stiffening capability. The pylons were modelled as uniform solid beam elements (beam4). The pylons and the backstays were fully-fixed at their connection to the foundations, and the bridge deck was also treated as fixed over a finite length at each end, based on observations from the site visit and in accordance with the relevant design drawings.

The parapets were modelled as structural parts, rather than simply as a distributed mass along the edges. It was deemed important to capture their actual function because their contribution to the modal stiffness of lightweight slender footbridges can be significant, depending on the degree of continuity achieved between the segments (Pimentel 1997, FIB 2005). The parapet parts were all treated as beam elements (beam4). Connections were incorporated into the handrails and footrails to allow them to move longitudinally, with two connections in each panel (between parapet posts), as in the constructed bridge. Two spring elements were used at each connection, one in the vertical and the other in the longitudinal direction. These allowed longitudinal movement, but provided rigid restraint in all other directions. The spring's stiffness could be adjusted accordingly once field data became available.

3.2 Preliminary study of FE model parameters (prior to testing)

The FE model described above was subjected to a modal analysis to determine the mode shapes and corresponding frequencies. These gave an initial indication of the dynamic characteristics of the footbridge.

The results of the modal analysis, however, obviously depend upon the input parameters used in the model, and to obtain accurate results it is necessary to match the mass and the stiffness of the structure. Several important parameters are either not possible to know (for example, the amount of pretension in the cables), or will not exactly match the values assumed during design or in manufacturers' data sheets (for example, the moduli of the GFRP pultruded deck components), or construction may deviate from the idealised assumptions in the model (for example, the boundary conditions).

It is well known that the effect of dead load and the effect of the initial cable tension (pretensioning) upon the structural stiffness are important in a modal analysis of a suspension bridge (Kim *et al.* 2012).

During installation of the Wilcott footbridge the deck self-weight (including the GFRP components, ballast and surfacing) was measured, and therefore the deck mass (including the parapets) in the model was adjusted to the estimated value of 26.5 tonnes.

A prestressed-modal analysis was performed in ANSYS, which involves two steps (Merce *et al.* 2007). Before the modal analysis, the cable pretension is set by running a static analysis step so that the structural members are stressed due to the dead load and initial cable tension (Ren *et al.* 2004).

Considering that dead load effects can be straightforward to apply, the results of the static analysis (herein deck deflection and cables' tension) are used to adjust the amount of pretensioning in the main cables by considering two factors: 1) minimum discrepancies between the deflected deck after the static analysis and the initially unloaded deck and 2) the tension in the cables, satisfying the designers' calculations. Both requirements were met through a trial-and-error iterative process in which increasing cable pretensioning results in a deck deflection decrease.

The results from the preliminary modal analysis were used to plan the field test. The calculated natural frequencies indicated that the footbridge had many modes below 10Hz, which informed the frequency ranges to be studied, and consequently the required sampling rate. The calculated mode shapes were used to identify the optimum locations for the accelerometers to accurately capture the modes of interest; this was particularly important for the location of the stationary accelerometer, which (as described below) was placed to avoid as many modal nodes as possible.

4. Vibration testing

4.1 Test procedure

The Wilcott footbridge is rather isolated, with only sporadic crossings. Dynamic motion of the bridge is excited by pedestrians, wind, and uplift resulting from large vehicles passing beneath the bridge. It was decided to focus on quantifying vertical motion of the bridge deck, based upon the FE analysis, preliminary on-site observations, and to make efficient use of the time available on site. The FE analysis indicated that the first torsional mode occurred above 5Hz and so is not of concern according to Eurocode 0 (EN1990 2002), which only recommends assessing torsional modes with natural frequencies less than 2.5Hz.

The response of the footbridge was recorded (a) as vehicles passed beneath the bridge, (b) due to walking at a set frequency controlled by a digital metronome, and (c) stamping at a set frequency at the antinode of the mode being investigated.

A variety of methods can be used for the vibration testing of structures. The most appropriate method depends upon the type of structure, the available equipment, and the operational conditions (Cunha *et al.* 2012). "Output-only" analyses are based only on response (output) data, with no record of the excitation (input) force. These analyses are primarily used for ambient vibration surveys (AVS), but there are cases where human activities can be used as the excitation (Farrar *et al.* 1999). The structure remains functional during AVS tests, because the ambient vibrations are recorded in the structure's normal operating environment. The AVS method was consequently chosen for the field test on the Wilcott footbridge, based also upon information from previous tests on FRP footbridges (Pimentel 1997, Bai and Keller 2008, Stratford 2012). The influence of pedestrian mass on the footbridge was not considered during the tests due to the absence of traffic across the bridge.

Two accelerometers were used during the tests, which were placed on the centre-line of the bridge to record the vertical vibration modes. One of the accelerometers was placed at a fixed reference station, positioned to avoid as many modal nodes as possible according to the FE analysis. The second was a roving accelerometer, placed at each of the thirteen measurement locations shown in Fig. 6. Ten of the measurement locations were at the hanger to deck connections, with one at mid-span, and the remaining two points between the last hanger and abutment at either end of the bridge. This arrangement yielded thirteen datasets of paired measurements, between every location and the reference station (point R in Fig. 6), and allowed the vertical mode shapes to be evaluated. This arrangement would yield information only for the dynamic characteristics in the vertical direction for the reasons quoted above. To examine the lateral direction the orientation of the uniaxial accelerometers should be adjusted along the centre-line, whereas the examination of the torsional modes requires a different set-up with accelerometers located at both edges of the deck.

The equipments used for the test comprised a four channel dynamic signal analyser (LDS Dactron Phaser), two high sensitivity uniaxial accelerometers suitable for low frequency measurements and battery amplifier units to raise the signal level. A sampling frequency of 23Hz was chosen for the AVS test, so as to capture the first eight vertical modes of the bridge (which had been shown to occur in the range 0 to 10Hz during the initial FE modal analysis), with anti-aliasing filter cut off frequency of about 0.45 of the sampling frequency. For tests involving pedestrian activity, the sampling frequency was adjusted to comply with the requirements set in the literature (Griffin 1990) which suggests at least a sampling frequency of 20 times the pacing rate used by the pedestrian during the test. The acquisition parameters are listed in Table 1.

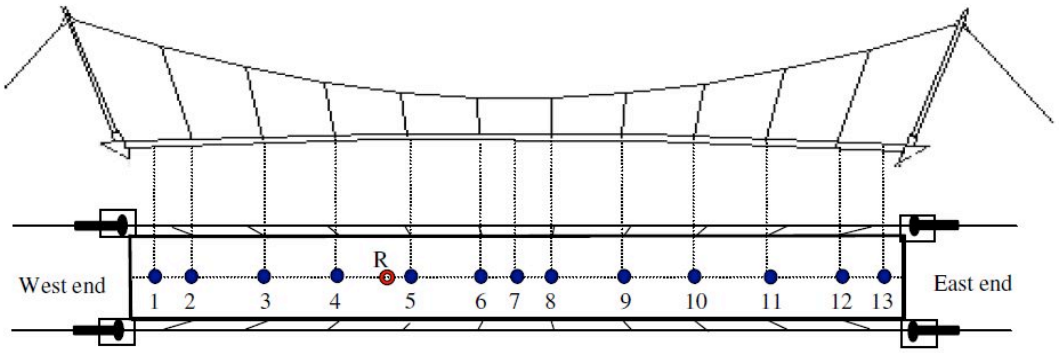

Fig. 6 The accelerometer locations used to obtain measurements, shown schematically on a plan and elevation of the bridge (R = fixed reference station)

Table 1. The data acquisition parameters.

Parameter	Type	Value
Accelerometer sensitivity	Roving accelerometer (PCB model 393B12)	9570 mV/g
	Stationary accelerometer (PCB model 355B04)	1029 mV/g
Sampling frequency (f_s)	Ambient test	23 Hz
	Pedestrian test	$f_s > 20 \times f_p$ (f_p: pacing rate used in test) f_s (V2)=40Hz and f_s (V3)=50Hz
Temperature	Ambient	14°C

4.2 Overall observations during the field test

During the field tests there were noticeable vertical vibrations due to pedestrian excitation, with clear peaks in the dynamic response at 1.5Hz and 2.2Hz, corresponding to the second vertical (V2) and third vertical (V3) modes predicted prior to testing using the FE model.

It was also observed that walking at a pacing rate of 2.2Hz caused the cables to oscillate laterally at half this frequency. Walking at 2.2Hz results in both vertical excitation and a smaller lateral excitation at 1.1Hz, and the FE model showed that the first local cable vibration mode is at around 1Hz, making them prone to vibration by walking.

The 1.5Hz (V2) and 2.2Hz (V3) vibration modes were targeted for further investigation as they correspond to the normal walking frequency range from 1.4 to 2.4Hz. Tests were conducted at frequencies controlled by metronome to investigate these modes, by both walking across the bridge, and by stamping at an antinode of the vibration mode, and results were recorded after excitation had stopped to allow damping to be assessed.

The passage of large Heavy Goods Vehicles beneath the bridge caused noticeable vertical vibration due to truck-induced wind gust, whereas smaller vehicles produced a barely perceptible response.

5. Data analysis

The acquired data were analysed to obtain the frequency response and to identify the vibration modes using the software Spice (Spice 1999; Peeters *et al.* 1999) and ARTeMIS (SVibS 2009). The vibration modes were initially identified using the simple peak-picking method (in Spice and ARTeMIS) and checked using the stochastic subspace identification (SSI) technique (in ARTeMIS). The following three sections describe (1) the vibration modes, (2) the damping, and (3) the peak accelerations recorded during the field tests.

5.1 Modal identification

The singular values of the spectral density matrices are shown in Fig. 7. This was obtained using data gathered from the reference station and the thirteen measurement points. Eight vertical vibration modes in the range 1 to 8Hz were obtained from the peaks in the PSD spectrum, and these are listed in Table 2. The damping ratios that are also listed in Table 2 are discussed in section 5.2.

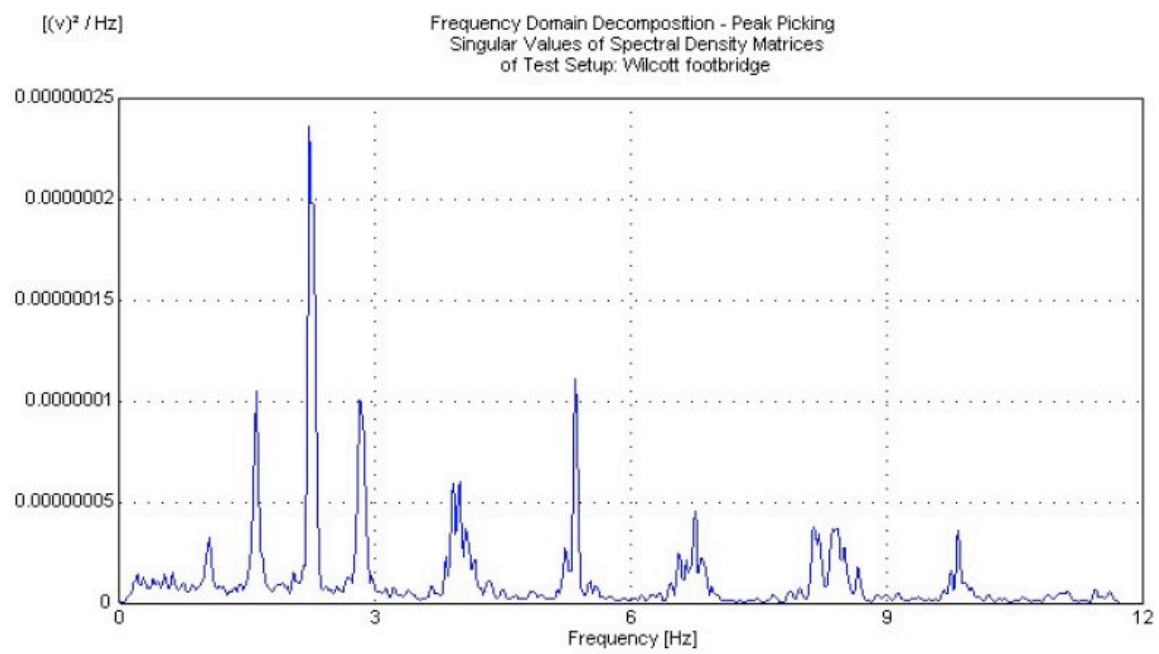

Fig. 7 The singular values of the spectral density matrices obtained from the field test.

Table 2. A summary of the modal parameters (frequency and damping) obtained from modal analysis.

No	Frequency (Hz)	Pedestrian tests Damping (ζ%)	
		Walking	Stationary stamping
V1	1.03	NM*	NM*
V2	1.55	1.64	1.84
V3	2.22	0.72	1.50
V4	2.77	NM*	NM*
V5	3.97		
V6	5.26		
V7	6.61		
V8	7.93		

*NM= Not Measured

The mode shapes for the first four vertical vibration modes (V1 to V4) are shown in Fig. 8, which compares the normalised mode shapes measured during the field test to their numerical counterparts from the updated FE model. The measured mode shapes and modal ordering agree with the modes predicted using the FE analysis, with modal assurance criterion (MAC) values around to 0.9, where unity corresponds to perfect correlation (Ewins 2000).

The first vertical mode (V1) is antisymmetric, followed by a symmetric second vertical mode

(V2), which is opposite to the modal ordering for a beam-like bridge. This modal ordering is expected for a suspension bridge, in which the first symmetric mode usually has stationary nodes on either side of the bridge (Brownjohn 1997).

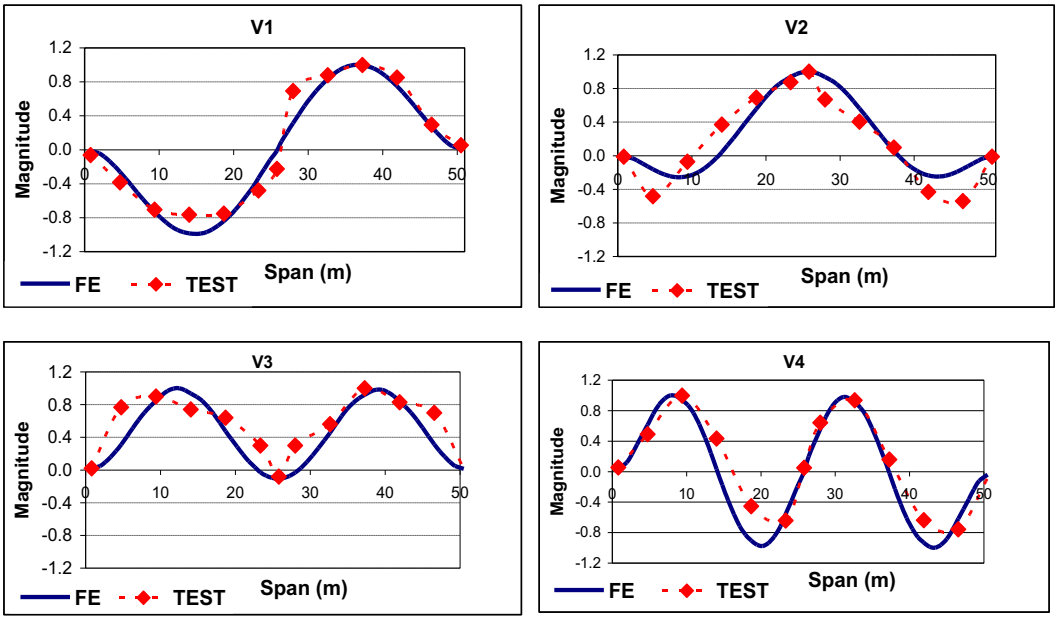

Fig. 8 A comparison of the first four normalised vertical mode shapes obtained from the tests to those obtained from the finite element model.

5.2 Damping measurements

The amount of damping in the Wilcott footbridge was measured for the second (V2) and third (V3) vertical vibration modes, because (as identified above), these occur within the normal walking frequency range. Damping was measured by two methods, following either walking or stamping excitation of the bridge. For the former method, a person walked across the bridge at either 1.5Hz (V2) or 2.2Hz (V3) using the digital metronome, and the decay in the bridge response after the person had left the bridge was used for the estimation. A typical decay response for the second vertical mode following walking excitation is shown in Fig. 9. The second method involved stamping at a set frequency at one point on the bridge, and then recording the decay response as the person stood still.

The logarithmic decrement method was used to quantify the damping from a response such as that in Fig. 9. For two successive peaks that are m cycles apart, the logarithmic decrement (δ) is calculated from the magnitude of the two peaks (x_n, x_{n+m}) using (Chopra 2007)

$$\delta = \frac{1}{m} \ln \frac{x_n}{x_{n+m}} \tag{1}$$

The damping ratio (ζ) was then calculated from the logarithmic decrement using

$$\zeta = \frac{1}{\sqrt{1 + \left(\frac{2\pi}{\delta}\right)^2}} \quad (2)$$

The measured damping ratio values from both the walking and stamping tests are summarised in Table 2. Greater damping was recorded during the stamping tests than during following walking for both of the vertical modes examined. This is usually the case for lightweight footbridges, due to the higher level of vibration caused by stamping or jumping compared to walking, together with the contribution of the people remaining on the bridge during the decay response (Georgakis and Jørgensen 2013, Sachse *et al.* 2003). In the present study one extra person remained on the footbridge following the stamping tests, whereas only the operator of the signal analyser was present on the bridge during the decay phase following the walking tests. Part of the difference in damping ratios between the walking and stamping tests is likely to be due to damping due to the person on the bridge, and part due to the greater level of vibration, but this was not examined.

The third vertical mode was less damped than the second mode (Table 2), and the difference is particularly large (around 50%) for the walking tests. As noted above, walking at 2.2Hz to excite the third vertical mode also excited lateral oscillation of the suspension cables at half this frequency, and consequently the decay response following walking for V3 is a combination of the decay of the vertical bridge mode and the lateral cable oscillation. Whilst the magnitude of the cable oscillation was not measured, it was in the order of 100mm, and consequently a large proportion of the vibration energy would have been in the cables, which were relatively undamped compared to vertical motion of the bridge deck. This was evident in the measured decay response, which had two parts: initially, at larger accelerations the decay was exponential, but at smaller amplitudes the rate of decay became constant, which is a sign of non-linearity consistent with the two modes that were decaying. Assessing damping by stamping did not generate cable oscillation, and this consequently had an exponential decay response and a larger value of damping.

The damping ratio associated with the first vertical mode excited by normal walking is usually used to benchmark damping between different bridges. For Wilcott this is 1.64% (for V2, at 1.55Hz), which is greater than damping ratios of around 0.8% for reported “lively” footbridges. A low damping ratio, however, does not of itself result in lively behaviour, and other “lively” footbridges have damping ratios over 1.5%.

By way of comparison, the first vertical mode of the all-FRP Aberfeldy cable-stayed footbridge was measured at 1.59Hz (in 1995, soon after it was constructed), with a damping ratio of 0.84%. However, the damping ratio had decayed to only 0.4% by 2000, which is believed to be due to degradation of the FRP parapet system that had been designed to provide frictional damping (Stratford, 2012). Wilcott footbridge has a stainless steel mesh cable parapet that contributes to the bridge damping, and will not deteriorate in the same manner.

Typical values for footbridges constructed from concrete and steel are shown in Table 3, from measurements on UK beam-type footbridges excited to resonance by a single pedestrian (Pretlove 1995) and from the value suggested in the UK bridge code, BS5400 for design “*in the absence of more precise of information*” (BS5400 2006).

Damping in footbridges is a subject under constant examination, and there is little data available on the amount of damping in FRP footbridges, although damping is vital in the evaluation of their dynamic behaviour. The Wilcott measurements will consequently be useful in future design.

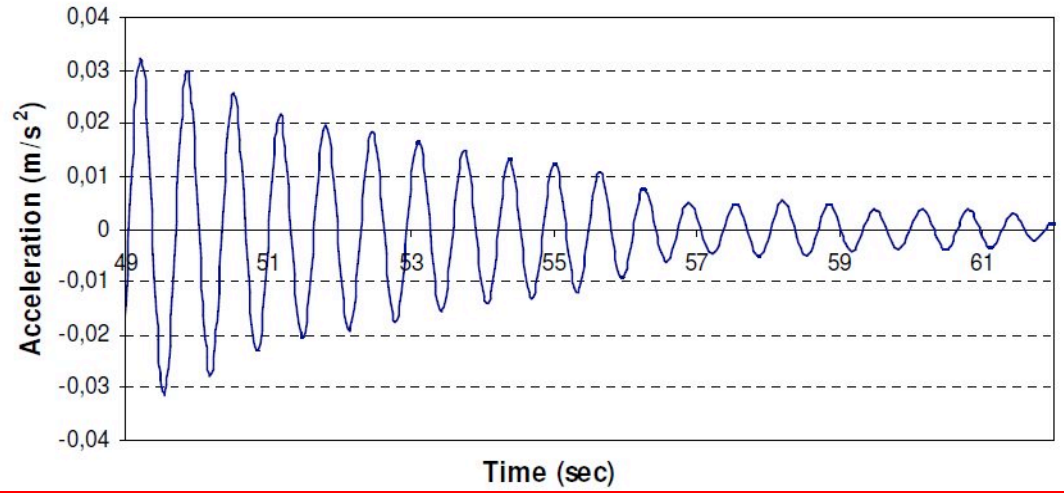

Fig. 9 The decay response of the second vertical mode (V2) after walking at 1.5 Hz.

Table 3. Damping ratios (ζ%) for typical beam-type footbridges.

Construction material	Pretlove (1995)			BS5400 (2006)
	Min.	Mean	Max.	
RC	0.8	1.3	2.0	0.8
Prestressed	0.5	1.0	1.7	-----
Steel-concrete composite construction	0.3	0.6	-----	0.65
Steel	0.2	0.4	-----	0.5

5.3 Peak accelerations

The dynamic serviceability assessment of the footbridge was completed by estimating the peak accelerations during the two walking tests at 1.5Hz (V2) and 2.2 Hz (V3). This was measured from the acceleration-time history of the footbridge at the antinode of the excited node. The objective of these walking tests was to compare the measured accelerations with the acceptability limits defined by the UK bridge code BS5400 (2006) and Eurocode 0 (EN1990 2002).

Two crossings were performed for each mode using the same pedestrian. A typical example of

the time-history response for walking at 1.5Hz is shown in Fig. 10, recorded at mid-span. The acceleration response increases until it reaches a maximum when the pedestrian reaches the centre of the bridge (the antinode of mode V2, see Fig. 8). The acceleration drops when the pedestrian approaches the modal nodes and diminishes when the pedestrian leaves the bridge deck at 49s.

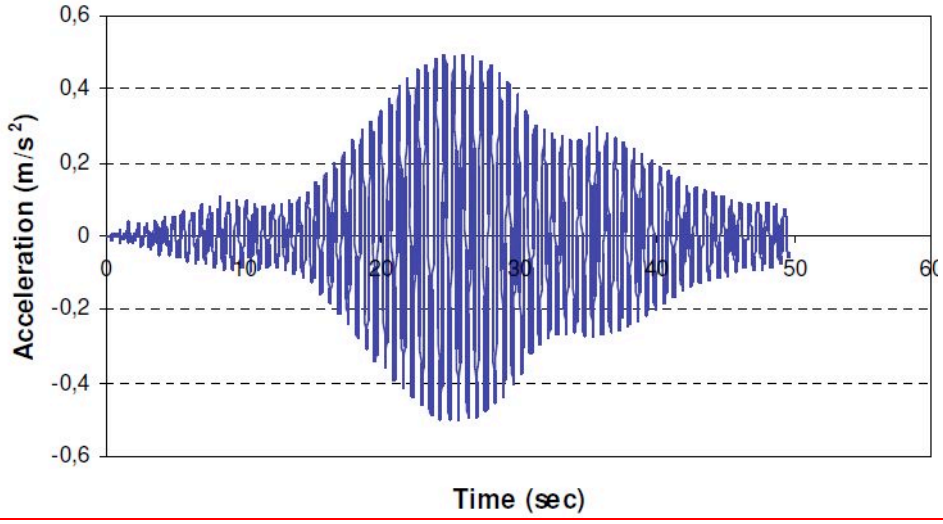

Fig. 10 The acceleration response at mid-span measured during walking at 1.5 Hz

Table 4 summarises the peak accelerations measured for modes V2 and V3, and compares these to the acceptability limits in BS5400 and Eurocode 0. V2 gave the higher peak acceleration, but in both cases the peak accelerations were below the acceptability limits. However, the bridge has only been tested with a single pedestrian, and additional tests could be performed, including (for example) normal and synchronised walking tests with different sized pedestrian groups, as well as running and jumping activities (Van de Broeck *et al.* 2011, Gudmudsson *et al.* 2008).

The footbridge also has modes at higher frequencies of 2.8Hz (V4) and 4.0Hz (V5) (see Table 2) that might be excited by pedestrian activities such as running and the second harmonic of walking respectively. Runners are unlikely to be able to maintain the required frequency along the whole length of the bridge under normal conditions (without the use of a digital metronome), and will only take a short time to cross the bridge. It is possible that organised events such as marathons might be of concern (SETRA 2006). Whilst there have been some reported cases of footbridge excitation due to the second harmonic of pedestrian excitation (Ivorra *et al.* 2015. Brownjohn and Fu 2005), preliminary on-site trials (prior to taking measurements) demonstrated that the lower modes V2 and V3 had the maximum amplitude.

Table 4. Comparison of the measured peak accelerations due to walking against design code acceptability limits.

Mode	Frequency	Measured peak acceleration (m/s^2)	Acceptable peak acceleration (m/s^2)	
			BS5400 (2006)	Eurocode 0 (EN1990 2002)
V2	1.5 Hz	0.47	0.62	0.7
V3	2.2 Hz	0.21	0.75	0.7

6. Finite element model updating

Finite element updating improves the correlation between a numerical model and test data (Zhang *et al* 2009, Sousa *et al.* 2014). Inaccuracies in the results from a model are usually due to the simplifying assumptions, or uncertainties in geometry, material properties, or boundary conditions (Zivanovic *et al.* 2007). The finite element model described in section 3 was used to predict the dynamic behaviour of the bridge prior to the field test. After the test had been conducted, the finite element was updated using a sensitivity analysis (in Excel) and the optimisation tools provided within ANSYS.

An initial sensitivity analysis was performed to determine the effect of several parameters upon the FE model results (Votsis 2007). This identified the parameters that have the greatest effect upon the dynamic characteristics of the bridge, and these were studied in the updating procedure:

1. the orthotropic properties of the bridge GFRP deck, (i.e. the longitudinal elastic modulus E_x, the transverse and vertical moduli $E_y = E_z$, and the shear modulus G
2. the density of the GFRP deck;
3. the elastic modulus of the suspension and hanger cables;
4. the amount of initial strain in the cable members; and
5. the overall stiffness of the handrails based on the connectivity and continuity between the individual panels.

Table 5 lists the values of the key parameters before and after the updating procedure.

Table 5. Modifications of the model parameters by finite element updating

Parameter		Initial Value	Updated Value
Deck longitudinal elastic modulus	E_x, GPa	21	23.8
Deck transverse moduli	E_y=E_z, GPa	10	9
Deck shear modulus	G, GPa	9	11
Density	kg/m^3	1930	1930
Hangers	E_x, GPa	200	199
Main cables	E_x, GPa	150	165

The updating procedure demonstrated that the structure's dynamic response is sensitive to the performance of the parapet system. The lower natural frequencies were nearly trebled in the case whereas the parapets segments are fully continuous and rigidly connected throughout rather than modelling the parapets as simple attachments on the deck, made from individual panels with no connection between them. Thus to achieve the correct stiffness of the structure, the stiffness of the spring elements was varied between these two extremes (rigid connection/no connection) during the updating process to reach a value that represents the actual connectivity of the parapets.

After the implementation of the updating procedure the FE model values closely matched their experimental counterparts as shown in Table 6 using the MAC criterion for the correlation of the mode shapes and the percentage differences for the frequencies.

Table 6. List of frequencies and correlation of values obtained from testing and FE updating

No	FE model (prior testing and updating)	Measured Frequency (Hz)	FE model-updated values	% Frequencies difference	MAC Values
V1	0.92	1.03	1.02	-0.19	0.94
V2	1.38	1.55	1.53	-1.03	0.86
V3	2.06	2.22	2.22	-0.05	0.87
V4	2.48	2.77	2.79	0.84	0.89
V5	3.61	3.97	4.01	0.93	0.89
V6	4.80	5.26	5.30	0.63	0.89
V7	6.05	6.61	6.72	1.63	0.81
V8	7.01	7.93	7.76	-2.04	0.79
L1	1.48	---	1.58	---	---
L2	4.17	---	4.42	---	---
T1	5.02	---	5.34	---	---
T2	5.25	---	5.56	---	---

The FE model updating process produced a numerical model that accurately simulates the structural behaviour of the Wilcott footbridge. This is very important especially for asset management reasons. In the case of a future dynamic testing within the context of an inspection routine, the updated FE model can be employed in a condition assessment to investigate any possible deviation between the two sets of measurements i.e. to examine and provide the reasons causing the changes in the dynamic characteristics. This concept can be applied for any future occasional or planned periodic monitoring.

Also, the updated FE model can be used to simulate possible damage scenarios on the footbridge and investigate how possible deterioration e.g. bonding degradation, can affect the performance of the footbridge and the safety of the users (Votsis *et al.* 2005).

If deemed necessary it can be used to improve the vibration serviceability of the Wilcott footbridge or more importantly the behaviour of similar footbridges. This can be achieved by investigating further the contribution of parapets and also through modifications in the use of the ballast material. The updated model can be used to simulate the pedestrian excitation using the

relevant modelling guidelines in the current Standards. Through this process, the applicability, suitability and accuracy of these Standards regarding FRP footbridges can be evaluated.

7. Conclusions

The dynamic performance of the Wilcott footbridge was assessed through a combination of field tests and finite element modelling. The modal properties of the first eight vertical modes were extracted from the results of the test using signal processing and stochastic subspace identification techniques. The acquired data and the subsequent analysis show that AVS is suitable and can be successfully used for the dynamic investigation of a FRP footbridge.

The fundamental vertical frequency at 1.03 Hz is in line with current trends found in slender footbridges. This vibration mode was not examined further as it cannot be excited by pedestrians.

The remaining measured modes range up to 8 Hz. Furthermore the correlation of the extracted six first mode shapes with their numerical counterparts produced high MAC values although the limited measured points affected the MAC values of modes V7 and V8. Nevertheless, if better quality shapes are required for advanced analysis, improved quality can be achieved by increasing the number of the measurement locations.

Damping values were obtained for the second (V2) and third (V3) vertical modes, which are the most important for the footbridge's vibration serviceability assessment, as they lie within the normal walking range. The damping was estimated through walking and stamping tests using the logarithmic decrement method; higher values were obtained by the stamping test which confirms the dependency of damping on vibration magnitude. The measured values are comparatively higher than those measured on lively footbridges. It was observed that dynamic cable/deck interaction during the investigation of mode V3 had a marked effect on damping as the cables' oscillation introduced non-linearities to the expected exponential form of the response decay.

Furthermore, in the context of the vibration serviceability, pedestrian walking tests were carried out. For the Wilcott footbridge, modes V2 and V3 can be excited by normal walking. The results of pedestrian tests showed that V2 exhibits the larger response but both modes result in values smaller than the respective acceleration limit set in the current standards. Additional tests employing other forms of pedestrian activities such as running and groups of pedestrians will help to provide a more solid assessment on the footbridge's serviceability status. Also the influence of pedestrian mass on footbridge frequencies and damping will provide useful insight into the human-structure interaction on lightweight FRP footbridges.

The field data were also used to update the developed FE model. An important result was that the contribution of parapets to the stiffness of slender footbridges is very important and their effect should not be neglected; they can indeed be utilized as structural elements to increase stiffness and reduce excessive vibrations. Also for suspension bridges the amount of initial strain in the cables is very important for the accurate representation of overall stiffness.

The updated FE model can be used in further sensitivity studies and can also be used as a benchmark to assess durability influences that might arise as a result of the bridge's exposure to the environment (e.g. moisture uptake). This belongs to the damage assessment area which is supported by periodic monitoring data to quantify deterioration which at the initiation stage cannot be identified by visual inspection but only when serious damage is present e.g. bonding degradation.

In this respect, a repeat visit to the footbridge in the future, if possible concurrently with a principal inspection, would be beneficial in improving our understanding of the dynamic properties of FRP bridges during their service lives.

At the moment, where limited information exists on the long-term performance and behaviour of FRP bridges such data are vital for an effective design and accurate numerical analysis and assessment.

Acknowledgments

The authors would like to thank Professor Shun-ichi Nakamura and Mr John Cadei for fruitful discussions on design aspects and valuable feedback on the organisation of the field test. We are grateful to the Highways Agency (Mr Neil Louden) and to Balfour Beatty for kindly allowing us to perform the field study on the bridge.

References

Alampalli, S. and Washer, G.A. (2013), Part VI: Nondestructive Testing and Evaluation, in: *The International Handbook of FRP Composites in Civil Engineering*, ed. Zoghi M, CRC Press.

ANSYS (Analysis System) (2003), *ANSYS user's manual v.8.0*. Houston, U.S.

Bachmann, H. (2002), "Lively footbridges- a real challenge", *Proceedings of the International Conference on the Design and Dynamic Behaviour of Footbridges*, Office Technique pour l'Utilisation de l'Acier (OTUA), Paris, France, November.

Bai, Y., and Keller, T. (2008), "Modal parameter identification for a GFRP pedestrian bridge", *Compos. Struct*. , **82**(1), 90-100.

Bakis, C.E., Bank, L.C., Brown, V.L., Cosenza, E., Davalos, J.F., Lesko, J.J., Machida, A., Rizkalla, S.H. and Triantafillou, T.C. (2002), "Fiber-reinforced polymer composites for construction - State-of-the-Art review*", J. Compos. Constr.,* **6**(2), 73-87.

Barker, C., DeNeumann, S., Mackenzie, D. and Ko, R. (2005), "Footbridge pedestrian vibration limits, Part 1: Pedestrian input", *Footbridge 2005*

Brownjohn, J.M.W. (1997) "Vibration characteristics of a suspension footbridge", *J Sound Vib.,* **202**(1), 29-46.

Brownjohn, J.M.W. and Fu, T.N. (2005), "Vibration Excitation and Control of a Pedestrian Walkway by Individuals and Crowds", *Shock Vib.,* **12** (5), 333-347.

BS5400 (2006), *Steel, concrete and composite bridges - Part 2: Specification for loads*, British Standards Institution, U.K.

Cadei, J. (2003), *The Nesscliffe Bypass Wilcott Footbridge- a Triumph of FRP,* Concrete, June.

Chopra, A.K. (2007), *Dynamics Of Structures-Theory And Applications To Earthquake Engineering*, Pearson-Prentice Hall, New Jersey, USA.

Cunha, A., Caetano, E., Magalhães, F., and Moutinho C. (2012), "Recent perspectives in dynamic testing and monitoring of bridges*", Struct. Control Hlth*, **20**(6), 853–877.

Dallard, P., Fitzpatrick, A.J., Flint A., Le Bouvra, S., Low A., Smith, R.M. and Willford, M. (2001), "The london millennium footbridge", *The Struct. Eng*., **79**(22), 17-33.

EN1990 (2002), *Basis of structural design*, Eurocode 0, European Committee for Standardization, Brussels.

EN1995 (2004), *Design of timber structures–Part 2: Bridges*, Eurocode 5, European Committee of Standardization, Brussels.

Ewins, D.J. (2000), *Modal Testing: Theory, Practice and Applications*, 2nd edition, Research Studies Press, Baldock, U.K.

Farrar, C.R., Duffey, T.A., Cornwell, P.J. and Doebling, S.W. (1999), "Excitation methods for bridge structures", *Proceedings of the 17th International Modal Analysis Conference (IMAC),* Society for Experimental Mechanics, Kissimmee, Florida, USA, February.

FIB (International Federation for Structural Concrete) (2005), *Guidelines for the Design Of Footbridges*, FIB Bulletin 32, November.

Fujino, Y., Pacheco, B.M., Nakamura, S. and Warnitchai, P. (1993), "Synchronization of human walking observed during lateral vibration of a congested pedestrian bridge", *Earthq. Eng. and Struct. Dyn.*, **22**, 741-758.

Georgakis, C.T. and Jørgensen, N.G. (2013), "Change in mass and damping on vertically vibrating footbridges due to pedestrians", *Proceedings of the 31st IMAC*, New York, February.

Griffin, M.J. (1990), *Handbook of Human Vibration*, Academic Press, London, U.K.

Gudmundsson, G., Ingolfsson, E.T., Einarsson, B., and Bessason, B. (2008), "Serviceability assessment of three lively footbridges in Reykjavic", *Proceedings of the International Conference on Footbridges 2008*, Porto, Portugal, July.

Hivoss (Human induced Vibrations of Steel Structures) (2008), "Design of footbridges-Background document", RFS2-CT-2007-00033, Research Fund for Coal and Steel.

Hollaway, L.C. and Head, P.R. (2001), *Advanced Polymer Composites and Polymers in the Civil Infrastructure*, Elsevier, Oxford, U.K.

Ivorra, S., Foti, D., Bru, D. and Baeza, F. (2015), "Dynamic Behaviour of a Pedestrian Bridge in Alicante, Spain", *J. Perform. Constr. Facil*., **29**(5).

Keller, T. (2003), *Use of Fibre Reinforced Polymers in Bridge Construction*, International Association for Bridge and Structural Engineering, Structural Engineering Documents, IABSE: SED7, Zurich, Switzerland.

Kim, H.K., Kim, N.S., Jang, J.H. and Kim, Y.H. (2012), "Analysis model verification of a suspension bridge exploiting configuration survey and field-measured data", *J. Bridge Eng*., **17**(5), 794-803.

Matsumoto, Y., Nishioka, T., Shiojiri, H., and Matsuzaki, K. (1978), "Dynamic design of footbridges", *IABSE Periodica*.

Merce, R. N., Doz, G. N., Vital de Brito, J. L., Macdonald, J. H. G. and Friswell, M. I. (2007), "Finite element model updating of a suspension bridge using ANSYS software", *Proceedings of Inverse Problems, Design and Optimization Symposium*, Miami, Florida, U.S.A, 16-18 April.

Pachi, A. and Ji, T. (2005), "Frequency and velocity of people walking", *The Struct. Eng.,* **83**(2),36-40.

Peeters, B., Van den Branden, B., Laquière, A. and De Roeck, G. (1999), "Output-only modal analysis: development of a GUI for Matlab", *Proceedings of the 17th IMAC*, Kissimmee, Florida, USA, February.

Pimentel, R.L. (1997), "Vibrational performance of pedestrian bridges due to human-induced loads." Ph.D. Dissertation, University of Sheffield. Sheffield, UK.

Pretlove, A.J., Rainer, J.H. and Bachmann, H. (1995), "Pedestrian bridges", *Vibration Problems in Structures: practical guidelines - Chapter: Vibrations induced by people*, eds Bachmann et al., Zurich.

Ren, W.X., Blandford, G.E. and Harik, I.E. (2004), "Roebling suspension bridge, Part I: Finite-element model and free vibration response", *J. of Bridge Eng*., **9**(2), 110-118.

Sachse, R., Pavic, A. and Reynolds, P. (2003), "Human-structure dynamic interaction in civil engineering dynamics: A literature review", *The Shock and Vibration Digest*, **35**(1), 3-18

SETRA (Technical Department for Transport, Roads and Bridges Engineering and Road Safety) (2006), "Assessment of vibrational behaviour of footbridges under pedestrian loading." Footbridges Technical Guide, Paris, France.

Sousa, H., Bento J. and Figueiras J. (2014), "Assessment and management of concrete bridges supported by monitoring data-based Finite Element modelling", *J. Bridge Eng*, **19**(6).

SPICE (Signal Processing in Civil Engineering) (1999), "SPICE v.2", K.U.Leuven – Structural Mechanics.

Stratford, T. (2012), "The condition of the Aberfeldy footbridge after 20 years of service", *14th International Conference on Structural Faults and Repair*, Edinburgh. July.

Strongwell Corporation (2010), “COMPOSOLITE-Fiberglass Building Panel System.” Bristol, Virginia, USA.

SVibS (Structural Vibration Solutions) (2009), “ARTeMIS Extractor Pro”.

Van den Broeck, P., Van Nimmen, K., Gezels, B., Reynders, E. and De Roeck, G. (2001), “Measurements and simulation of the human-induced vibrations of a footbridge”, *Proceedings of the International Conference on Structural Dynamics EURODYN2011*, Leuven, Belgium, July.

Votsis, R.A., Wahab M.M.A. and Chryssanthopoulos. M.K. (2005), "Simulation of damage scenarios in an FRP composite suspension footbridge", *Key Eng. Mat.* , **293**, 599-606

Votsis, R.A. (2007), “Vibration Assessment of FRP Composite Pedestrian Bridges”, Ph.D. Dissertation, University of Surrey, Guildford.

Willford, M. (2002), “Dynamic actions and reactions of pedestrians”, *Proceedings of the International conference on the Design and Dynamic Behaviour of Footbridges*, Paris, France, November.

Zhang, K., Duan, Z. and Liu, Y. (2009). “Dynamic Parameters identification and finite element model updating for continuous rigid frame bridge”, *J. Highway Transp. Res. Dev*., **4**(1), 53-59.

Živanović, S., Pavic, A. and Reynolds, P. (2005), “Vibration serviceability of footbridges under human-induced excitation: a literature review”, *J Sound Vib*., **279** (1–2), 1-74.

Živanović, S., Pavic, A. and Reynolds, P. (2007), “Finite element modelling and updating of a lively footbridge: The Complete Process”, *J Sound Vib*., **301** (1-2), 126-145.

Fig. 1. An overview of the completed Wilcott footbridge.

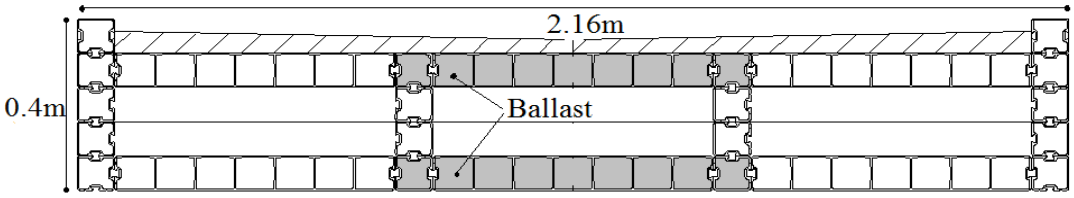

Fig. 2. A cross-section through the bridge deck.

Fig. 3. Fabrication of the GFRP bridge deck, showing the configuration of the transverse beams.

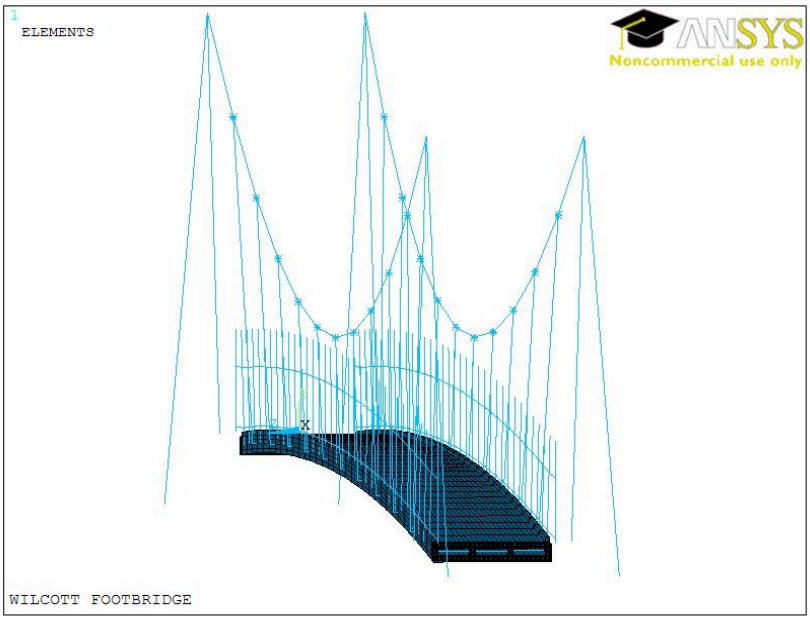

Fig. 4. An overview of the finite element model of the bridge.

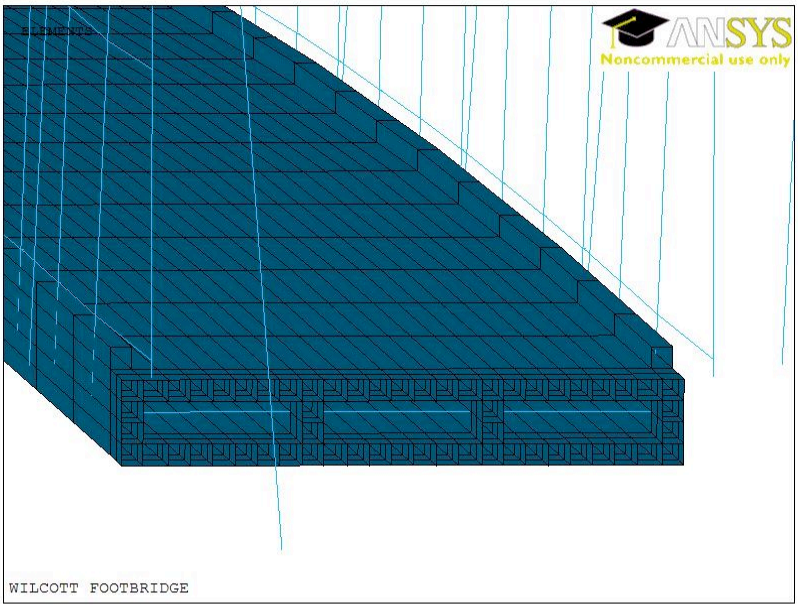

Fig. 5. A detailed view of the GFRP modular deck within the model.

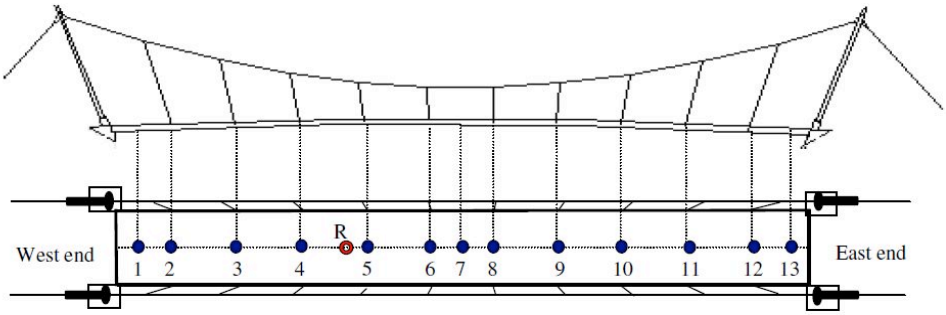

Fig. 6. The accelerometer locations used to obtain measurements, shown schematically on a plan and elevation of the bridge (R=reference station)

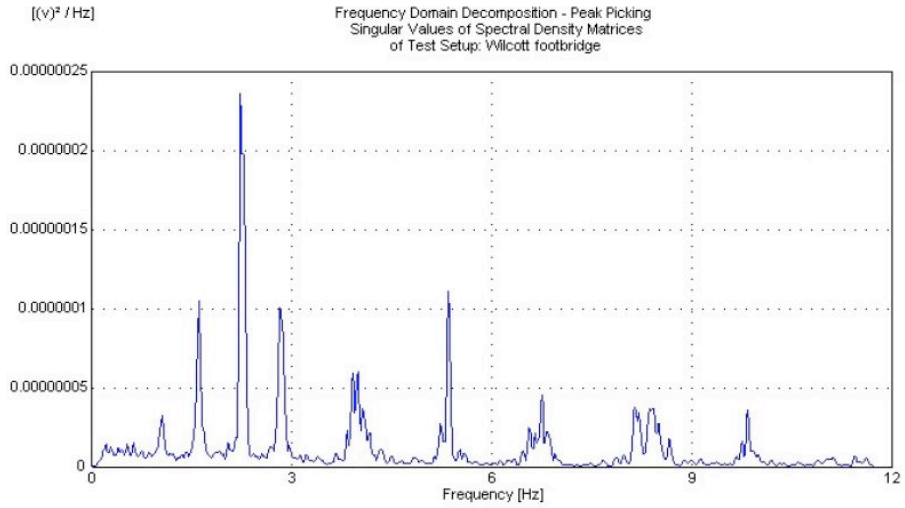

Fig. 7. The singular values of the spectral density matrices obtained from the field test.

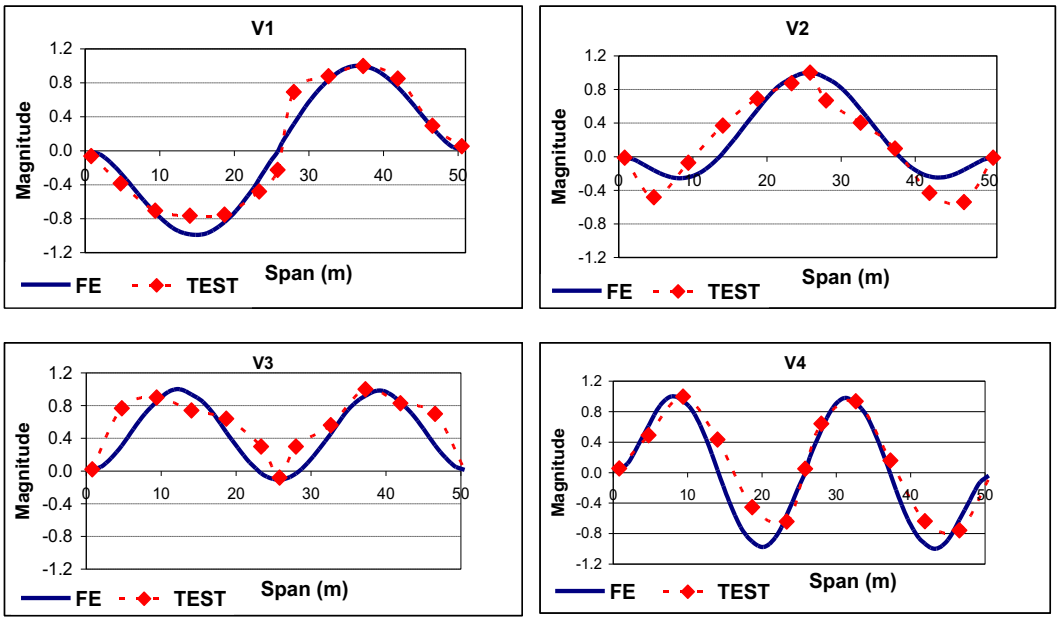

Fig. 8. A comparison of the first four normalised vertical mode shapes obtained from the tests to those obtained from the finite element model

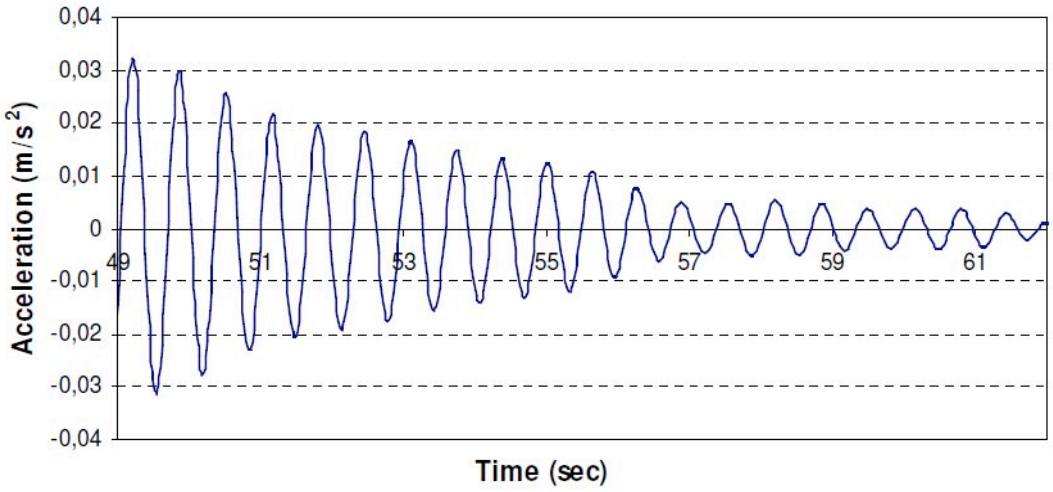

Fig. 9. The decay response of the second vertical mode (V2) after walking at 1.5 Hz.

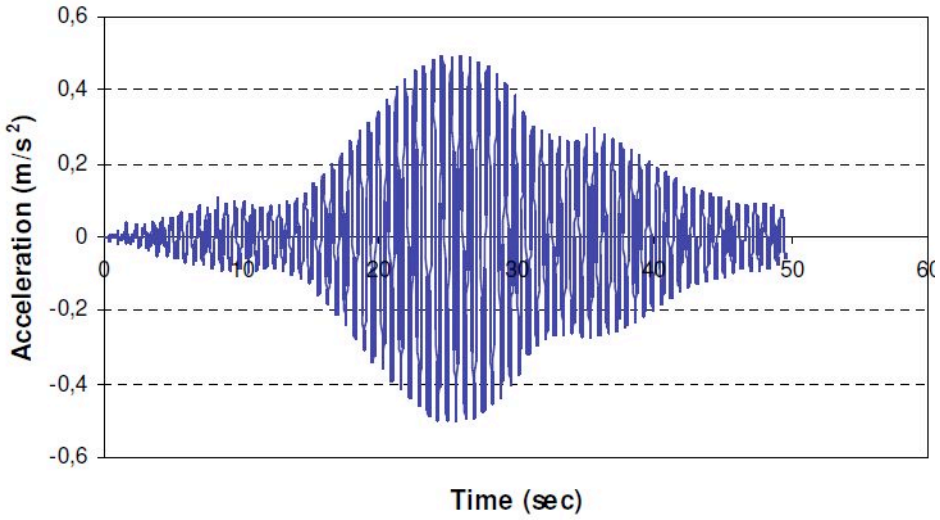

Fig. 10 The acceleration response at mid-span measured during walking at 1.5 Hz

Table 1. The data acquisition parameters.

Parameter	Type	Value
Accelerometers sensitivity	Roving accelerometer (PCB model 393B12)	9570 mV/g
	Stationary accelerometer (PCB model 355B04)	1029 mV/g
Sampling frequency (f_s)	Ambient test	23 Hz
	Pedestrian test	f_s >20 x f_p (f_p: pacing rate used in test) f_s (V2)=40Hz and f_s (V3)=50Hz
Temperature	Ambient	14°C

Table 2. A summary of the modal parameters (frequency and damping) obtained from modal analysis.

No	Frequency (Hz)	Pedestrian tests Damping (ζ%)	
		Walking	Stationary Stamping s/s
V1	1.03	NM*	NM*
V2	1.55	1.64	1.84
V3	2.22	0.72	1.50
V4	2.77	NM*	NM*
V5	3.97		
V6	5.26		
V7	6.61		
V8	7.93		

*NM= Not Measured

Table 3. Damping ratios (ζ%) for typical beam-type footbridges.

Construction material	Pretlove (1995)			BS 5400 (2006)
	Min.	Mean	Max.	
RC	0.8	1.3	2.0	0.8
Prestressed	0.5	1.0	1.7	-----
Steel-concrete composite construction	0.3	0.6	-----	0.65
Steel	0.2	0.4	-----	0.5

Table 4. Comparison of the measured peak accelerations due to walking against design code acceptability limits.

Mode	Frequency	Measured peak acceleration (m/s^2)	Acceptable peak acceleration (m/s^2)	
			BS5400 (2006)	Eurocode 0 (EN1990 2002)
V2	1.5 Hz	0.47	0.62	0.7
V3	2.2 Hz	0.21	0.75	0.7

Table 5. Modifications of the model parameters by finite element updating.

Parameter		Initial Value	Updated Value
Deck longitudinal elastic modulus	E_x, GPa	21	23.8
Deck transverse modulii	E_y=E_z, GPa	10	9
Deck shear modulus	G, GPa	9	11
Density	kg/m^3	1930	1930
Hangers	E_x, GPa	200	199
Main cables	E_x, GPa	150	165

Table 6. List of frequencies and correlation of values obtained from testing and FE updating

No	FE model (prior testing and updating)	Measured Frequency (Hz)	FE model-updated values	% Frequencies difference	MAC Values
V1	0.92	1.03	1.02	-0.19	0.94
V2	1.38	1.55	1.53	-1.03	0.86
V3	2.06	2.22	2.22	-0.05	0.87
V4	2.48	2.77	2.79	0.84	0.89
V5	3.61	3.97	4.01	0.93	0.89
V6	4.80	5.26	5.30	0.63	0.89
V7	6.05	6.61	6.72	1.63	0.87
V8	7.01	7.93	7.76	-2.04	0.86
L1	1.48	---	1.58	---	---
L2	4.17	---	4.42	---	---
T1	5.02	---	5.34	---	---
T2	5.25	---	5.56	---	---